



Published in final edited form as:

*Eur Radiol.* 2023 October ; 33(10): 6970–6980. doi:10.1007/s00330-023-09654-5.

## Co-existing intracranial and extracranial carotid atherosclerosis predicts large-artery atherosclerosis stroke recurrence: a single-center prospective study utilizing combined head-and-neck vessel wall imaging

Gemuer Wu<sup>1,2</sup>, Chengcheng Zhu<sup>3</sup>, Huiying Wang<sup>4</sup>, Dingwei Fu<sup>5</sup>, Xiudi Lu<sup>6</sup>, Chen Cao<sup>7</sup>, Xianchang Zhang<sup>8</sup>, Jinxia Zhu<sup>8</sup>, Lixiang Huang<sup>1</sup>, Mahmud Mossa-Basha<sup>3</sup>, Shuang Xia<sup>1</sup>

<sup>1</sup>Department of Radiology, Tianjin First Central Hospital, School of Medicine, Nankai University, No. 24 Fukang Road, Nankai District, Tianjin 300192, China

<sup>2</sup>Department of Radiology, Affiliated Hospital of Inner Mongolia Medical University, Hohhot 010050, China

<sup>3</sup>Department of Radiology, University of Washington, 325 9Th Ave, Seattle, WA 98104, USA

<sup>4</sup>The School of Medicine, Nankai University, 94 Weijin Road, Tianjin 300071, China

<sup>5</sup>Department of Radiology, The Second Affiliated Hospital of Wannan Medical College, 10 Kangfu Road, Jinghu District, Wuhu 241000, China

<sup>6</sup>Department of Radiology, First Teaching Hospital of Tianjin University of Traditional Chinese Medicine, National Clinical Research Center for Chinese Medicine Acupuncture and Moxibustion, Tianjin 300381, China

<sup>7</sup>Department of Radiology, Tianjin Huanhu Hospital, Tianjin 300350, China

<sup>8</sup>MR Collaboration, Siemens Healthineers Ltd., Beijing, China

✉ Shuang Xia, xiashuang77@163.com.

Gemuer Wu and Chengcheng Zhu contributed equally to this study as co-first authors.

**Supplementary Information** The online version contains supplementary material available at <https://doi.org/10.1007/s00330-023-09654-5>.

Compliance with ethical standards

**Guarantor** The scientific guarantor of this publication is Shuang Xia.

**Statistics and biometry** No complex statistical methods were necessary for this paper.

**Informed consent** Written informed consent was provided by all participants or their authorized proxy.

**Ethical approval** Institutional review board approval was obtained.

Methodology

- Prospective study
- Observational
- Performed at one institution

**Conflict of interest** Authors Xianchang Zhang and Jinxia Zhu are employees of Siemens Healthineers. The remaining authors declare no relationships with any companies whose products or services may be related to the subject matter of the article.

Springer Nature or its licensor (e.g. a society or other partner) holds exclusive rights to this article under a publishing agreement with the author(s) or other rightsholder(s); author self-archiving of the accepted manuscript version of this article is solely governed by the terms of such publishing agreement and applicable law.

## Abstract

**Objectives**—Intracranial and extracranial plaque features on high-resolution vessel wall imaging (HR-VWI) are associated with large-artery atherosclerosis (LAA) stroke recurrence. However, most studies have focused on a single vascular bed, and the prognostic value of combined intracranial and extracranial plaque features has yet to be studied. This study aimed to investigate the roles of plaque features, plaque number, and co-existing atherosclerosis in predicting stroke recurrence, utilizing combined head-and-neck HR-VWI.

**Methods**—From September 2016 to March 2020, participants with acute LAA ischemic strokes were prospectively enrolled and underwent combined head-and-neck HR-VWI. The participants were followed for stroke recurrence for at least 12 months or until a subsequent event occurred. The imaging features at baseline, including conventional and histogram plaque features, plaque number, and co-existing atherosclerosis, were evaluated. Univariable Cox regression analysis and the least absolute shrinkage and selection operator (lasso) method were used for variable screening. Multivariable Cox regression analyses were used to determine the independent risk factors of stroke recurrence.

**Results**—A total of 97 participants ( $59 \pm 12$  years, 63 men) were followed for a median of 30.9 months, and 21 participants experienced recurrent strokes. Multivariable Cox analysis identified co-existing intracranial high signal on T1-weighted fat-suppressed images (HST1) and extracranial carotid atherosclerosis (HR, 6.12; 95% CI, 2.52–14.82;  $p = 0.001$ ) as an independent imaging predictor of stroke recurrence.

**Conclusion**—Co-existing intracranial HST1 and extracranial carotid atherosclerosis independently predicted LAA stroke recurrence. Combined head-and-neck HR-VWI is a promising technique for atherosclerosis imaging.

**Clinical relevance statement**—This prospective study using combined head-and-neck HR-VWI highlighted the necessity of both intracranial culprit plaque evaluation and multi-vascular bed assessment, adding value to the prediction of stroke recurrence.

## Keywords

Ischemic stroke; Recurrence; Atherosclerosis; Magnetic resonance imaging; Vessel wall imaging

---

## Introduction

Intracranial and extracranial large-artery atherosclerosis (LAA) is the primary cause of ischemic stroke in Asia [1]. Furthermore, recent studies have shown that co-existing intracranial and extracranial LAA is prevalent in stroke patients (59.3–77.6%) [2, 3], and intracranial and carotid stenosis was associated with future cardiovascular events [1]. These findings highlight the need for simultaneous evaluation of both intracranial and extracranial vasculature to improve stroke risk stratification.

High-resolution vessel wall imaging (HR-VWI) has unique advantages over traditional angiographic imaging methods, providing in vivo visualization of plaque composition [4, 5]. However, outward remodeling can frequently result in the underestimation of plaque burden due to minimal stenosis, even in the setting of advanced plaque [5, 6]. Previous studies

demonstrated that many high-risk plaque features, including a high signal on T1-weighted fat-suppressed images (HST1) [7, 8], positive remodeling [7], plaque enhancement [9], and plaque burden [10], were associated with stroke events. However, most previous studies separately focused on either extracranial carotid or intracranial plaque imaging. Few studies evaluated extracranial and intracranial plaques simultaneously, possibly due to a lack of appropriate imaging methods such as combined head-and-neck HR-VWI [2].

In addition, longitudinal studies investigating the prognostic value of combined head-and-neck VWI for predicting recurrent stroke still need to be completed. Whether combined head-and-neck VWI can better predict recurrent stroke than sole imaging of extracranial or intracranial plaques is unknown.

Our study aimed to determine the extracranial and intracranial plaque features that could predict recurrent stroke using combined head-and-neck VWI and quantitative histogram image analysis [11].

## Materials and methods

### Study patients

This prospective, single hospital-based study was approved by the local institutional ethics committee. All participants or their authorized proxies provided written informed consent. Consecutive adult participants with acute ischemic stroke were prospectively recruited from September 2016 to March 2020. Inclusion criteria were (1) adult participants; (2) acute ischemic stroke confirmed by DWI in the unilateral anterior circulation, unilateral posterior circulation, and basilar artery territory; (3) MRI scans performed within 30 days after symptom onset, and completion of all sequences during the same scan session for each participant; and (4) intracranial LAA was considered the stroke etiology after multidisciplinary consultation (Supplemental material) [12]. Exclusion criteria were (1) nonatherosclerotic intracranial or extracranial arterial disease; (2) cardio-embolic risk factors; (3) reperfusion treatment of index strokes (intravenous thrombolysis/endovascular thrombectomy/angioplasty/stenting); (4) angioplasty/stenting/carotid endarterectomy during follow-up; (5) malignant tumor history or newly diagnosed malignant tumors during follow-up; or (6) poor imaging quality or incomplete clinical data.

The demographic and clinical information, including sex, age, vascular risk factors, previous stroke history, symptom onset to HR-VWI interval, laboratory blood tests, medications, and the National Institutes of Health (NIH) Stroke Scale on admission, was collected.

### Image protocol

The MRI was performed on a 3-T scanner (MAGNETOM Prisma, SIEMENS Healthcare) using a 64-channel head-and-neck coil. The protocol included DWI, T2 fluid-attenuated inversion recovery imaging, time-of-flight magnetic resonance angiography, dynamic susceptibility contrast perfusion-weighted imaging, and pre- and post-contrast 3D HR-VWI. HR-VWI was performed using an inversion recovery prepared sampling perfection with application-optimized contrast using different flip angle evolutions (IR-SPACE) [13, 14] in a sagittal plane optimized for plaque evaluation and flow signal suppression. The

scan covered the whole brain and was at least 2 cm below the common carotid artery bifurcation. The post-contrast scan was performed with the same protocol after the perfusion imaging (gadobenate dimeglumine, 0.1 mmol/kg, 2 mL/s, Bracco Sine Pharmaceutical). The scanning parameters are shown in S. Table 1.

### Image analysis

Two readers with 8 and 6 years of experience in neuroradiology, respectively, performed image measurements and were blinded to the participants' clinical information. The plaque volume was semiautomatically measured using commercial analysis software, ITK-SNAP 3.8.0 ([www.itksnap.org](http://www.itksnap.org)) [15]. ImageJ 1.52a (Wayne Rasband, NIH) was used for histogram analysis. Other factors such as the HR-VWI plaque features (degree of stenosis, plaque burden, presence of HST1, enhancement ratio, enhancement grading, arterial remodeling ratio, and eccentric index for intracranial plaques; also the degree of stenosis, maximal wall thickness, plaque area, plaque burden, and presence of intraplaque hemorrhage or lipid core for extracranial carotid plaques), plaque number, and co-existing atherosclerosis were measured using commercial software (RadiAnt DICOM Viewer 2020.1, Medixant Corp.). The pre- and post-contrast 3D HR-VWI images were automatically synchronized, and manual adjustment was performed if there were obvious slice mismatches.

### Plaque identification and classification

The following large-arterial segments were analyzed: internal carotid artery, anterior cerebral artery (A1–2), middle cerebral artery (M1–2), posterior cerebral artery (P1–2), basilar artery, and vertebral artery (V2–4). An atherosclerotic plaque was defined as a focal vessel wall thickening [9]. The culprit plaque was either the only plaque present and therefore considered responsible for downstream ischemic stroke or, with multiple plaques, considered the most stenotic plaque within the relevant vascular territory of the index stroke [9] (S. Figure 1). Any disagreements in culprit plaque identification were resolved by discussion and consensus under the guidance of a senior neuroradiologist with 22 years of experience.

### HR-VWI and histogram plaque feature evaluation

After the culprit plaque was identified, the reformatted axial images centered at the most stenotic site of the culprit plaques were provided for further measurement. The plaque boundaries were delineated slice by slice, and plaque volume was automatically outputted and recorded. The plaque was observed slice by slice on the pre- and post-contrast HR-VWI reformatted images to evaluate HST1 and plaque enhancement. The following features were measured (S. Figure 2 and S. Figure 3): plaque volume, degree of stenosis [16], plaque burden [17], presence of HST1 [18], enhancement ratio [10], enhancement grading [9, 19], arterial remodeling ratio [17], and eccentric index [20] (detailed in Supplemental material). In addition, histogram features of the culprit plaques including mean, standard deviation, minimal value, maximal value, median, skewness, kurtosis, and the coefficient of variation were recorded [11]. All features were standardized using the mean CSF value (level of the lateral ventricle, avoiding the choroid plexus).

The following parameters of the extracranial carotid plaques were measured: degree of stenosis [16], maximal wall thickness, plaque area, plaque burden [17], presence of intraplaque hemorrhage [18], and lipid core [21].

The different combinations of plaque numbers (continuous variable) were counted and recorded for each participant: (1) intracranial + extracranial carotid plaques; (2) intracranial enhanced + extracranial carotid plaques; and (3) intracranial HST1 + extracranial carotid plaques.

Co-existing atherosclerosis (dichotomous variable) for each participant was recorded:

1. Intracranial stenosis (> 50%) + extracranial carotid atherosclerosis (referring to the patient having both intracranial stenosis and extracranial carotid plaques, and intracranial stenosis referred to the presence of > 50% stenosis of any large-arterial segment mentioned above)
2. Intracranial + extracranial carotid atherosclerosis
3. Intracranial enhanced + extracranial carotid atherosclerosis
4. Intracranial HST1 + extracranial carotid atherosclerosis

The distribution and frequency of high-risk plaques (with plaque enhancement or HST1) were also analyzed. The plaques were considered separate if they were discontinuous and had a typical plaque-free arterial wall between them. Finally, a plaque involving two arterial segments was counted as two separate plaques.

### Follow-up and outcome assessment

Participants were followed for at least 12 months to assess stroke recurrence for a maximum of 48 months or until a recurrent stroke occurred. Recurrent ischemic stroke was defined as new neurological deficits lasting > 24 h after the index stroke, confirmed by neurological examination and neuroimaging. Participants were followed by telephone interviews or routine outpatient clinic visits, and those lost to follow-up were censored at the last contact time.

### Statistical analysis

The sample size calculations were performed with 0.8 power and at a 0.05 significance level [22–24]. The assumed measurement error was 10%, and the estimated difference between groups was 10%, with a recurrence rate of 20% [22]. Therefore, the estimated sample size was 80 participants, with sixteen recurrent stroke participants. Considering the participants lost at follow-up and the possibility that real-world recurrent strokes might be less common, our target recruitment was 100 participants.

The measurement reproducibility was evaluated with the intraclass correlation coefficient. Univariable analysis was performed using Student's *T* test, Mann–Whitney *U* test, or chi-squared test, as appropriate. Univariable Cox regression analysis and the least absolute shrinkage and selection operator (lasso) method were used for variable screening. The chosen variables were included in the multivariable Cox regression analysis to obtain

the independent features associated with stroke recurrence. Time-dependent ROC and AUC curves were also plotted. The Delong test was used for AUC comparisons. In addition, Kaplan–Meier analysis with the log-rank test was used to compare the stroke-free probability after the index stroke. The sensitivity analysis was also performed by identifying factors related to ipsilateral stroke recurrence. Two-tailed  $p < 0.05$  indicated statistical significance. Finally, SPSS Statistics software 24.0 (International Business Machines Corp.) and R statistical software 4.0.1 were used for statistical analysis and plotting.

## Results

### Participant characteristics

A total of 97 participants (mean age, 59 years  $\pm$  12; 63 men) were included in the final analysis (Fig. 1). The demographic and clinical characteristics are summarized in Table 1. Over a median follow-up time of 30.9 months, 21 participants experienced recurrent stroke events. Three participants experienced recurrence in different arterial territories to the index stroke event. The median stroke recurrence time was 10 (range, 1–30.8) months. No difference could be found in the baseline demographic and clinical information between the recurrent and non-recurrent participant groups (all  $p > 0.05$ ). One participant died of diabetes mellitus complications during the follow-up period, and another experienced cerebral hemorrhage.

The distribution and frequency of high-risk plaques are shown in S. Table 2. Again, the results indicated the uneven distribution in our cohort, primarily of the intracranial lesions.

### Imaging features between recurrent and non-recurrent stroke participants

The imaging features are summarized in Table 2 and S. Table 3. Compared with the non-recurrent stroke participants, recurrent participants had more intracranial plaques (median, 6 vs. 4 lesions,  $p = 0.001$ ), more intracranial enhanced plaques (median, 3 vs. 2 lesions,  $p = 0.046$ ), more intracranial plaques with HST1 (median, 1 vs. 1 lesion,  $p = 0.04$ ), more extracranial carotid plaques (median, 1 vs. 0 lesions,  $p = 0.03$ ), a higher total plaque number of the different combinations (all  $p < 0.05$ ), and a higher proportion of co-existing intracranial and extracranial atherosclerosis with the different combinations (all  $p < 0.05$ ). The recurrent stroke participants also had culprit plaques with a higher plaque burden (median, 84.00 vs. 69.35%,  $p < 0.001$ ) and a higher degree of stenosis ( $59.82 \pm 17.76\%$  vs.  $47.08 \pm 32.09\%$ ,  $p = 0.02$ ).

Other HR-VWI and histogram features of the culprit plaques were not significantly different between the two groups (all  $p > 0.05$ ). The HR-VWI features of extracranial carotid plaques showed no difference between the two groups (Table 3).

### Imaging features associated with stroke recurrence

Using univariable Cox regression analysis and lasso selection, plaque burden (HR, 1.66; 95% CI, 1.21–2.28;  $p = 0.002$ ), the total number of intracranial plaques (HR, 1.33; 95% CI, 1.09–1.62;  $p = 0.004$ ), co-existing intracranial stenosis ( $> 50\%$ ) and extracranial carotid atherosclerosis (HR, 4.89; 95% CI, 2.02–11.80;  $p < 0.001$ ), co-existing intracranial

enhanced and extracranial carotid atherosclerosis (HR, 2.88; 95% CI, 1.19–6.95;  $p = 0.02$ ), and co-existing intracranial HST1 and extracranial carotid atherosclerosis (HR, 5.88; 95% CI, 2.42–14.30;  $p < 0.001$ ) were identified as input imaging variables in the multivariable analysis (Table 4). The analysis showed that co-existing imaging markers intracranial HST1 and extracranial carotid atherosclerosis (HR, 6.12; 95% CI, 2.52–14.82;  $p = 0.001$ ) were independently associated with stroke recurrence (Table 4). In addition, the culprit plaque burden was marginally significant ( $p = 0.050$ ).

In addition, the AUC values of the final regression model were higher than 0.70 (Fig. 2). The extracranial carotid plaque number was associated with stroke recurrence in the univariable Cox analysis (HR, 1.74; 95% CI, 1.14–2.67;  $p = 0.01$ ). Hence, we plotted the time-dependent AUCs of the single markers and applied the DeLong test for AUC comparison (Fig. 3). The AUCs of co-existing atherosclerosis were higher than those of the extracranial carotid plaque number ( $p < 0.05$ ). Notably, the Kaplan–Meier curves showed that co-existing atherosclerosis's stroke-free probability was higher than that without ( $p < 0.001$ , Fig. 4). Representative cases are shown in Fig. 5.

The same analysis was performed as a sensitivity analysis to identify factors related to ipsilateral stroke recurrence (eighteen events). Among the variables included in the multivariable Cox analysis (S. Table 4), the pre-median value and HST1 might be intrinsically associated. The higher the pre-median value, the more components with high signal intensity. Residual collinearity remained between the pre-median value and HSTI because they likely represented the same plaque composition (hemorrhage) [25]. In addition, HST1 defined by a well-established method [26] was chosen to input into the final model. The results indicated that co-existing intracranial HST1 and extracranial carotid atherosclerosis remained statistically significant. In addition, the culprit plaque burden trended toward significance ( $p = 0.050$ ).

### Imaging features of recurrent stroke events in different arterial territories

Three participants experienced recurrent stroke events in different arterial territories. Based on the distribution of recurrent stroke, the possible culprit plaques were present on the baseline HR-VWI images (S. Table 5, Fig. 6).

### Reproducibility and post hoc sample size calculation

There was good inter-reader measurement agreement, with all intraclass correlation coefficients  $> 0.85$  and a maximal coefficient of variation of 10.8% (S. Table 6). A post hoc power analysis was conducted to detect a 10% difference with a measurement error of 10.8%. The required sample size was 95 patients. We included 97 participants with 21 recurrence events, and the sample size was sufficient to draw safe conclusions.

## Discussion

In this prospective study, we used combined head-and-neck HR-VWI to simultaneously evaluate the high-risk features of intracranial and extracranial carotid atherosclerotic plaques. We identified co-existing intracranial HST1 and extracranial carotid atherosclerosis as independent imaging predictors of stroke recurrence. The combined evaluation of

intracranial and extracranial atherosclerosis improved the prediction performance compared to the separate evaluation of extracranial carotid arteries. Our results highlighted the importance of performing combined head-and-neck HR-VWI and provided new insight into its value in stroke risk assessment.

Using combined head-and-neck HR-VWI, we found co-existing intracranial HST1 and extracranial carotid atherosclerosis are risk factors for stroke recurrence. Furthermore, our results showed that the vulnerable intracranial plaques (with HST1), even if not culprits, might represent the extensive involvement and instability of atherosclerosis. In addition, more extensive atherosclerosis might indicate a higher overall burden because this is a systematic disease [27].

Plaque involvement in multiple arterial beds provides many potential sources of plaque rupture and artery-to-artery embolism. The advancement of combined head-and-neck VWI has provided a unique opportunity to study intracranial and extracranial plaque features simultaneously. In a series of studies using 7-T MRI, the intracranial atherosclerotic burden was associated with clinical cerebrovascular risk factors [28] and several extracranial atherosclerotic markers [29]. In addition, a large-scale longitudinal study ( $n = 806$ ) using magnetic resonance angiography showed that co-existing intracranial and extracranial arterial stenoses were a predictor of stroke recurrence [1].

VWI is superior to angiographic imaging techniques because DSA can miss up to 26.1% of non-stenotic plaques [5], and our study included a significant proportion of plaques with mild to no stenosis (16.4% of intracranial plaques and 85.7% of extracranial plaques had < 30% stenosis).

Li et al [3] followed 150 acute stroke/TIA patients for an average of 12 months and found co-existing carotid plaque and intracranial stenosis predicted future cardiovascular events. Our results were consistent with those of Li and colleagues. We extended their findings, with several advantages: (1) Li and colleagues included stroke and TIA patients, while we only included those with acute stroke. TIA symptoms can frequently be non-specific, and the diagnostic accuracy was limited; (2) their study included recurrent stroke, TIA, and acute coronary syndromes as outcomes while we focused exclusively on recurrent stroke; and (3) Li and colleagues did not perform intracranial HR-VWI and only evaluated intracranial arterial stenosis on magnetic resonance angiography, while we performed combined head-and-neck HR-VWI and evaluated intracranial and extracranial plaque features. Although the plaque distribution in our population was intracranial-predominant, possibly due to the susceptibility of Chinese people to intracranial arterial stenosis with earlier onset age and higher prevalence [30], the AUC of the co-existing atherosclerosis model was higher than that of the extracranial carotid plaque number model. This result further demonstrated the incremental value of two vascular bed combined evaluations, consistent with a previous study [31].

Our study found that the association between the culprit plaque burden and stroke recurrence tended toward significance ( $p = 0.050$ ). A previous cross-sectional study also reported a higher plaque burden associated with stroke recurrence [10]. In addition, a longitudinal 2D



HR-VWI study found that the increase in plaque burden during the follow-up predicted recurrent stroke, but the baseline plaque burden did not [22]. Our result differed from the latter study, possibly because (1) we only included participants with acute ischemic strokes, while that study enrolled both stroke and TIA patients; (2) we analyzed plaques in the whole head-and-neck region with 3D HR-VWI, while that study only focused on plaque features in a single culprit plaque of the middle cerebral or basilar arteries; and (3) we excluded participants who underwent reperfusion/endovascular treatment to avoid intervention-related imaging changes, a procedure that was not mentioned in their study. These changes could have affected the interpretation of the plaque features. Although it was marginally significant, future more extensive studies with more homogeneous cohorts could confirm our findings.

The degree of stenosis is known to predict stroke recurrence [32]. In our study, this factor correlated significantly with stroke recurrence in the univariable Cox analysis. However, the associations did not persist in the multivariable analysis. One possible reason for this is that there was only a moderate degree of stenosis of the culprit plaques in our cohort ( $49.84 \pm 21.28\%$ ), and only 21.6% of plaques had severe stenosis ( $> 70\%$ ). Luminal stenosis did not account for outward remodeling plaque, which can be the predominant pattern, even with advanced plaques. We did find that the plaque burden was marginally associated with stroke recurrence in the multivariable analysis.

A recent meta-analysis showed that HST1 was a robust imaging biomarker of symptomatic intracranial plaques [7] and was found to be associated with neurological impairment in stroke patients [33]. However, it is still being determined whether HST1 is an independent predictor for recurrence due to the lack of prospective studies. Our univariable Cox regression analysis results showed that HST1 in the culprit plaque tended toward significance ( $p = 0.06$ ). Plaque enhancement was also reported as a marker of plaque vulnerability [7] and was related to arterial stenosis progression [34]. In our study, the proportion of enhanced plaques was relatively high, and no differences in culprit enhancement ratio ( $p = 0.56$ ) or plaque enhancement ( $p = 0.55$ ) were found between the two groups. This result was likely because the imaging analysis was conducted after the stroke events, and the short interval from symptom onset to HR-VWI (median, 10 days) also contributed to these results [35]. In addition, we also analyzed the recurrent stroke events in the ipsilateral vascular territories, and the results remained the same. Although HST1 was related to stroke recurrence, it was not an independent risk factor in our cohort. Future studies with a more homogenous cohort might be needed.

This study had several limitations. First, the findings were based on a single-center study design focusing on LAA stroke, which might not be generalizable to other countries or patient populations. Second, our study had a moderate sample size. Third, the definition of culprit plaque was based heavily on the degree of stenosis caused by atherosclerotic plaques. Moreover, we did not evaluate the atherosclerotic involvement of other arterial beds (such as the aortic arch or coronary and peripheral arteries), which are also associated with stroke recurrence [27].

In conclusion, co-existing intracranial HST1 and extracranial carotid atherosclerosis independently predicted stroke recurrence. Combined head-and-neck high-resolution vessel wall imaging is a promising technique for atherosclerosis imaging. It is more valuable for stroke recurrence prediction than an investigation of the extracranial vascular bed alone.

## Supplementary Material

Refer to Web version on PubMed Central for supplementary material.

## Funding

This work was supported by the Natural Scientific Foundation of China (NSFC) (Grant No. 82171916 to S. Xia) and the Natural Science Foundation of Tianjin (Grant No. 20JCQNJC01250 to C. Cao). This work was also funded by the Tianjin Key Medical Discipline (Specialty) Construction Project. Chengcheng Zhu was supported by United States National Institute of Health (NIH) grants R01HL162743 and R00HL136883.

## Abbreviations

<b>HR</b>	Hazard ratio
<b>HR-VWI</b>	High-resolution vessel wall imaging
<b>HST1</b>	High signal on T1-weighted fat-suppressed images
<b>LAA</b>	Large-artery atherosclerosis
<b>Lasso</b>	Least absolute shrinkage and selection operator
<b>SI</b>	Signal intensity
<b>TIA</b>	Transient ischemic attack

## References

1. Suo Y, Jing J, Pan Y et al. (2021) Concurrent intracranial and extracranial artery stenosis and the prognosis of transient ischaemic symptoms or imaging-negative ischaemic stroke. *Stroke Vasc Neurol* 6:33–40 [PubMed: 32792459]
2. Xu Y, Yuan C, Zhou Z et al. (2016) Co-existing intracranial and extracranial carotid artery atherosclerotic plaques and recurrent stroke risk: a three-dimensional multicontrast cardiovascular magnetic resonance study. *J Cardiovasc Magn Reson* 18:90 [PubMed: 27908279]
3. Li J, Li D, Yang D et al. (2020) Co-existing cerebrovascular atherosclerosis predicts subsequent vascular event: a multi-contrast cardiovascular magnetic resonance imaging study. *J Cardiovasc Magn Reson* 22:4 [PubMed: 31928532]
4. Mandell DM, Mossa-Basha M, Qiao Y et al. (2017) Intracranial vessel wall MRI: principles and expert consensus recommendations of the American Society of Neuroradiology. *AJNR Am J Neuroradiol* 38:218–229 [PubMed: 27469212]
5. Tian X, Tian B, Shi Z et al. (2021) Assessment of intracranial atherosclerotic plaques using 3D Black-Blood MRI: comparison with 3D time-of-flight MRA and DSA. *J Magn Reson Imaging* 53:469–478 [PubMed: 32864816]
6. Wang Y, Liu X, Wu X, Degnan AJ, Malhotra A, Zhu C (2019) Culprit intracranial plaque without substantial stenosis in acute ischemic stroke on vessel wall MRI: a systematic review. *Atherosclerosis* 287:112–121 [PubMed: 31254918]

7. Song JW, Pavlou A, Xiao J, Kasner SE, Fan Z, Messe SR (2021) Vessel wall magnetic resonance imaging biomarkers of symptomatic intracranial atherosclerosis: a meta-analysis. *Stroke* 52:193–202 [PubMed: 33370193]
8. Zhu C, Tian X, Degnan AJ et al. (2018) Clinical significance of intraplaque hemorrhage in low- and high-grade basilar artery stenosis on high-resolution MRI. *AJNR Am J Neuroradiol* 39:1286–1292 [PubMed: 29794236]
9. Qiao Y, Zeiler SR, Mirbagheri S et al. (2014) Intracranial plaque enhancement in patients with cerebrovascular events on high-spatial-resolution MR images. *Radiology* 271:534–542 [PubMed: 24475850]
10. Ran Y, Wang Y, Zhu M et al. (2020) Higher plaque burden of middle cerebral artery is associated with recurrent ischemic stroke: a quantitative magnetic resonance imaging study. *Stroke* 51:659–662 [PubMed: 31856694]
11. Shi Z, Li J, Zhao M et al. (2020) Quantitative histogram analysis on intracranial atherosclerotic plaques: a high-resolution magnetic resonance imaging study. *Stroke* 51:2161–2169 [PubMed: 32568660]
12. Gao S, Wang YJ, Xu AD, Li YS, Wang DZ (2011) Chinese ischemic stroke subclassification. *Front Neurol* 2:6 [PubMed: 21427797]
13. Fan Z, Yang Q, Deng Z et al. (2017) Whole-brain intracranial vessel wall imaging at 3 Tesla using cerebrospinal fluid-attenuated T1-weighted 3D turbo spin echo. *Magn Reson Med* 77:1142–1150 [PubMed: 26923198]
14. Yang Q, Deng Z, Bi X et al. (2017) Whole-brain vessel wall MRI: a parameter tune-up solution to improve the scan efficiency of three-dimensional variable flip-angle turbo spin-echo. *J Magn Reson Imaging* 46:751–757 [PubMed: 28106936]
15. Yushkevich PA, Piven J, Hazlett HC et al. (2006) User-guided 3D active contour segmentation of anatomical structures: significantly improved efficiency and reliability. *Neuroimage* 31:1116–1128 [PubMed: 16545965]
16. Barnett HJ, Taylor DW, Eliasziw M et al. (1998) Benefit of carotid endarterectomy in patients with symptomatic moderate or severe stenosis. North American Symptomatic Carotid Endarterectomy Trial Collaborators. *N Engl J Med* 339:1415–1425 [PubMed: 9811916]
17. Qiao Y, Anwar Z, Intrapromkul J et al. (2016) Patterns and implications of intracranial arterial remodeling in stroke patients. *Stroke* 47:434–440 [PubMed: 26742795]
18. Liu J, Balu N, Hippe DS et al. (2016) Semi-automatic carotid intraplaque hemorrhage detection and quantification on magnetization-prepared rapid acquisition gradient-echo (MP-RAGE) with optimized threshold selection. *J Cardiovasc Magn Reson* 18:41 [PubMed: 27430263]
19. van der Kolk AG, Zwanenburg JJ, Brundel M et al. (2011) Intracranial vessel wall imaging at 7.0-T MRI. *Stroke* 42:2478–2484 [PubMed: 21757674]
20. Yamagishi M, Terashima M, Awano K et al. (2000) Morphology of vulnerable coronary plaque: insights from follow-up of patients examined by intravascular ultrasound before an acute coronary syndrome. *J Am Coll Cardiol* 35:106–111 [PubMed: 10636267]
21. Zhu C, Sadat U, Patterson AJ, Teng Z, Gillard JH, Graves MJ (2014) 3D high-resolution contrast enhanced MRI of carotid atheroma—a technical update. *Magn Reson Imaging* 32:594–597 [PubMed: 24630443]
22. Shi Z, Li J, Zhao M et al. (2021) Progression of plaque burden of intracranial atherosclerotic plaque predicts recurrent stroke/transient ischemic attack: a pilot follow-up study using higher-resolution MRI. *J Magn Reson Imaging* 54:560–570 [PubMed: 33600033]
23. Whitley E, Ball J (2002) Statistics review 4: sample size calculations. *Crit Care* 6:335–341 [PubMed: 12225610]
24. Grothues F, Smith GC, Moon JC et al. (2002) Comparison of interstudy reproducibility of cardiovascular magnetic resonance with two-dimensional echocardiography in normal subjects and in patients with heart failure or left ventricular hypertrophy. *Am J Cardiol* 90:29–34 [PubMed: 12088775]
25. Chen XY, Wong KS, Lam WW, Ng HK (2014) High signal on T1 sequence of magnetic resonance imaging confirmed to be intraplaque haemorrhage by histology in middle cerebral artery. *Int J Stroke* 9:E19 [PubMed: 24798044]

26. Wu F, Song H, Ma Q et al. (2018) Hyperintense plaque on intracranial vessel wall magnetic resonance imaging as a predictor of artery-to-artery embolic infarction. *Stroke* 49:905–911 [PubMed: 29540606]
27. Hoshino T, Sissani L, Labreuche J et al. (2018) Prevalence of systemic atherosclerosis burdens and overlapping stroke etiologies and their associations with long-term vascular prognosis in stroke with intracranial atherosclerotic disease. *JAMA Neurol* 75:203–211 [PubMed: 29279888]
28. Lindenholtz A, van der Kolk AG, van der Schaaf IC et al. (2020) Intracranial atherosclerosis assessed with 7-T MRI: evaluation of patients with ischemic stroke or transient ischemic attack. *Radiology* 295:162–170 [PubMed: 32013790]
29. Zwartbol MHT, Geerlings MI, Ghaznawi R, Hendrikse J, van der Kolk AG, Group U-SS (2019) Intracranial atherosclerotic burden on 7T MRI is associated with markers of extracranial atherosclerosis: the SMART-MR Study. *AJNR Am J Neuroradiol* 40:2016–2022 [PubMed: 31806592]
30. Leng X, Hurford R, Feng X et al. (2021) Intracranial arterial stenosis in Caucasian versus Chinese patients with TIA and minor stroke: two contemporaneous cohorts and a systematic review. *J Neurol Neurosurg Psychiatry*. 10.1136/jnnp-2020-325630
31. Li D, Dai W, Cai Y et al. (2018) Atherosclerosis in stroke-related vascular beds and stroke risk: a 3-D MR vessel wall imaging study. *Ann Clin Transl Neurol* 5:1599–1610 [PubMed: 30564625]
32. Kasner SE, Chimowitz MI, Lynn MJ et al. (2006) Predictors of ischemic stroke in the territory of a symptomatic intracranial arterial stenosis. *Circulation* 113:555–563 [PubMed: 16432056]
33. Liu S, Tang R, Xie W et al. (2021) Plaque characteristics and hemodynamics contribute to neurological impairment in patients with ischemic stroke and transient ischemic attack. *Eur Radiol* 31:2062–2072 [PubMed: 32997174]
34. Lu M, Zhang H, Liu D et al. (2022) Vessel wall enhancement as a predictor of arterial stenosis progression and poor outcomes in moyamoya disease. *Eur Radiol*. 10.1007/s00330-022-09223-2
35. Kwee RM, Qiao Y, Liu L, Zeiler SR, Wasserman BA (2019) Temporal course and implications of intracranial atherosclerotic plaque enhancement on high-resolution vessel wall MRI. *Neuroradiology* 61:651–657 [PubMed: 30834465]

**Key Points**

- This study highlighted the necessity of both intracranial culprit plaque evaluation and multi-vascular bed assessment, adding value to the prediction of stroke recurrence.
- This prospective study using combined head-and-neck HR-VWI found co-existing intracranial HST1 and extracranial carotid atherosclerosis to be independent predictors of stroke recurrence.

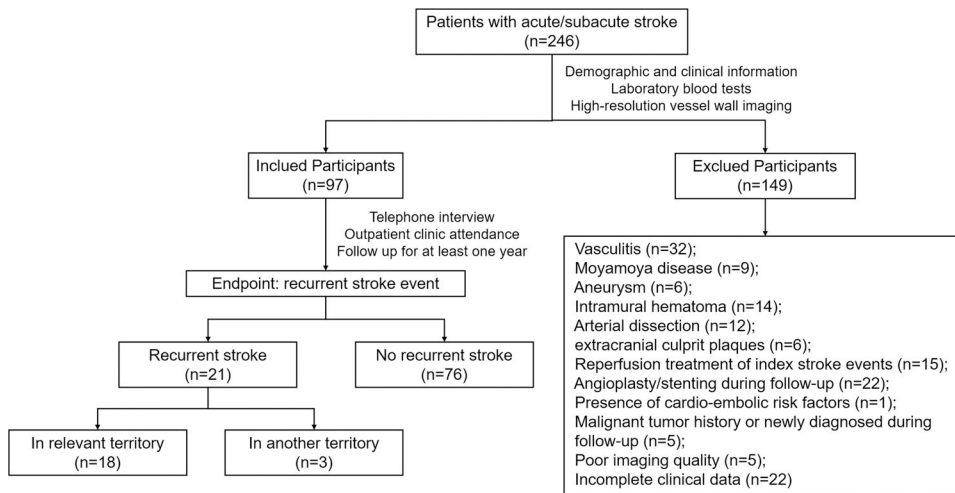


**Fig. 1.**  
Selection flow chart of the study sample

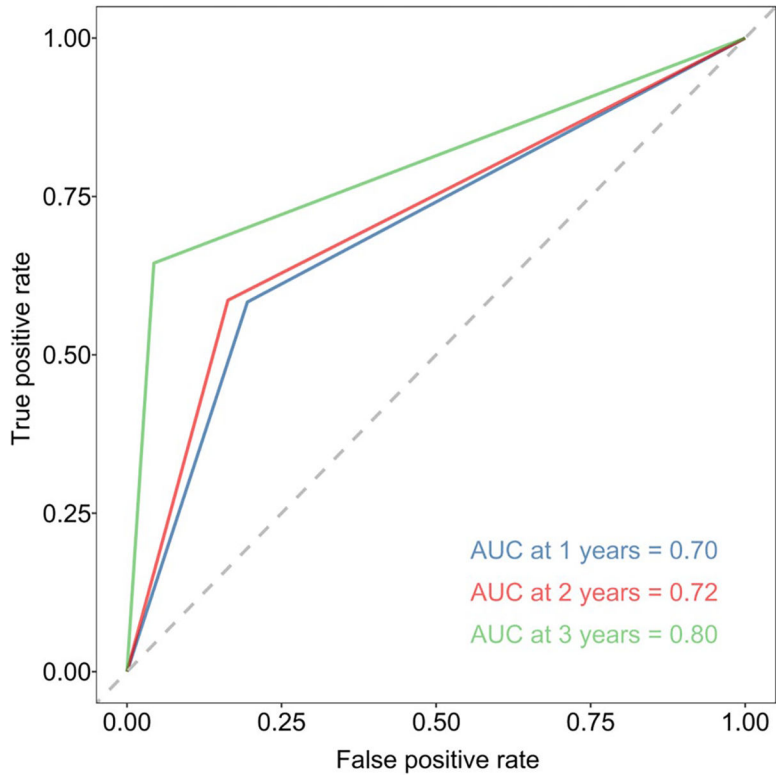


**Fig. 2.** Time-dependent ROC curves of the final Cox model identified by multivariable Cox regression analysis to predict stroke recurrence. The corresponding AUC values at 1, 2, and 3 years are also shown. All values > 0.70

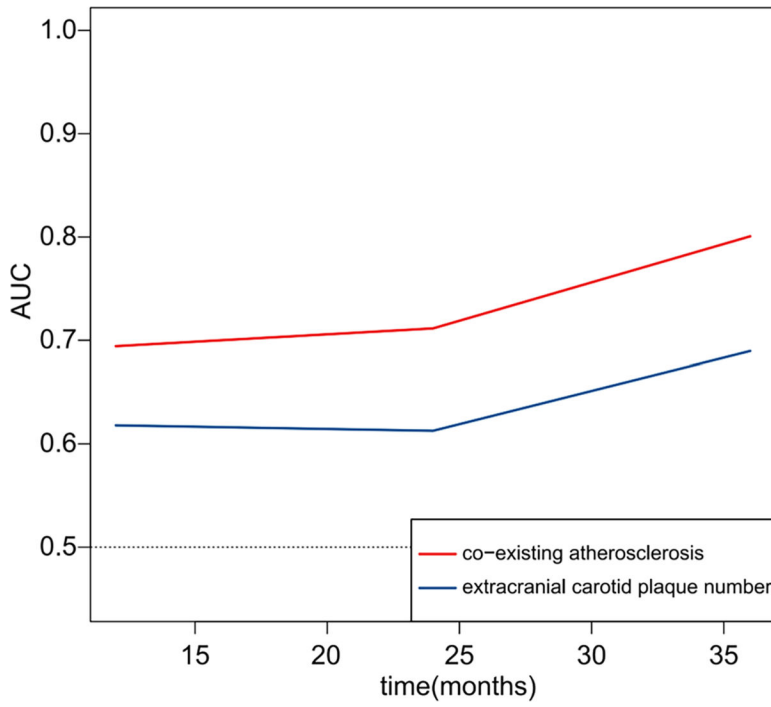


**Fig. 3.** Time-dependent AUC curves of the final Cox model (co-existing intracranial HST1 and extracranial carotid atherosclerosis) and extracranial carotid plaque number are shown. The AUC of the atherosclerosis was larger than 0.70 at every time point and performed better than the other variables



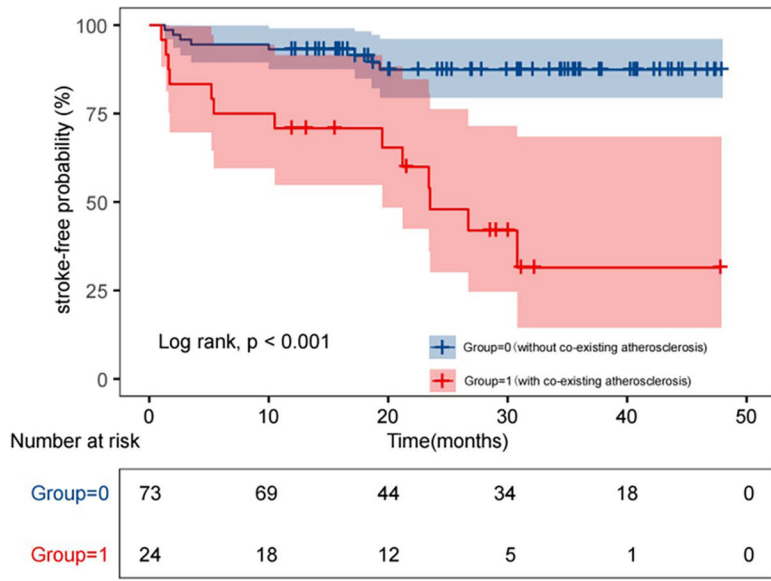


**Fig. 4.** Kaplan–Meier curves of stroke recurrence probability between patients with and without co-existing atherosclerosis during follow-up

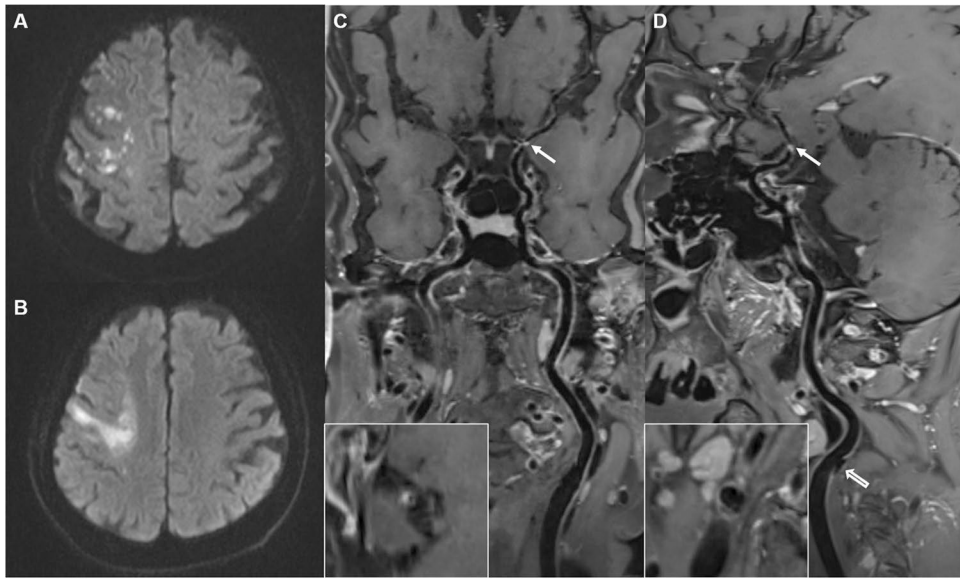


**Fig. 5.**

A 59-year-old woman presented with left limb weakness for 13 h. MRI (**A**, **C**, **D**) was performed 8 days after symptom onset. She suffered a recurrent event 35 days later, and diffusion-weighted imaging (**B**) was performed. Diffusion-weighted imaging (axial plane) (**A**) at baseline indicates scattered high signal intensity in the right frontal lobe. The curved multi-planar reconstruction image of post-contrast HR-VWI (**C**) shows the culprit plaque located in the initial part of the right middle cerebral artery (arrow). The curved multi-planar reconstruction image of post-contrast HR-VWI (**D**) also shows plaque located in the extracranial right internal carotid artery (hollow arrow); the local enlarged image shows the plaque with a high proportion of calcification and an irregular surface. Diffusion-weighted imaging (axial plane) (**B**) indicates strip-like high signal intensity in the right frontal lobe consistent with a recurrent stroke event

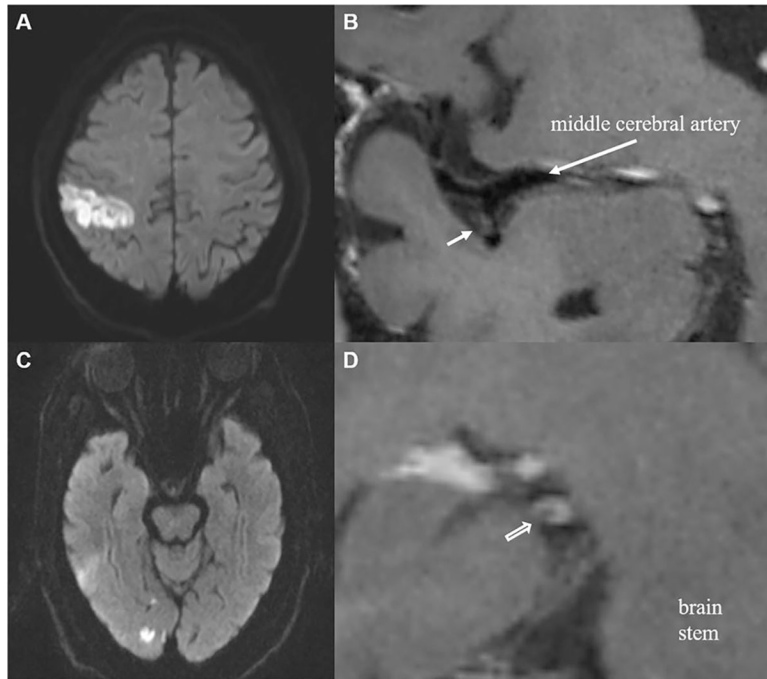


**Fig. 6.**

A 71-year-old man presented with left limb weakness for 7 h. MRI (**A**, **B**, **D**) was performed 3 days after symptom onset. She suffered a recurrent event 23.5 months later, and DWI (**C**) was performed. Diffusion-weighted imaging (axial plane) (**A**) at baseline indicates strip-like high signal intensity in the right frontal-parietal lobe. The multi-planar reconstruction image of post-contrast HR-VWI (**B**) shows the culprit plaque located in the M2 segment of the right middle cerebral artery (short arrow). Diffusion-weighted imaging (axial plane) (**C**) indicates high signal intensity in the right occipital lobe consistent with a recurrent stroke event. The multi-planar reconstruction image of post-contrast HR-VWI (**D**) also shows plaque located in the P1 segment of the posterior cerebral artery (hollow arrow), which might be the culprit plaque of the recurrent event

Table 1

## Participant demographics and clinical information

Variables	All participants (n = 97)	Recurrent participants (n = 21)	Non-recurrent participants (n = 76)	p value <sup>b</sup>
Age, years, mean (SD)	59 (12)	58 (9)	59 (12)	0.47
Male, n (%)	63 (64.9)	13 (61.9)	50 (65.8)	0.74
Hypertension, n (%)	86 (88.7)	19 (90.5)	67 (88.2)	>0.99
SBP, mm/Hg, median (IQR)	152 (27)	150 (17)	153 (31)	0.27
DBP, mm/Hg, median (IQR)	87 (18)	87 (19)	87 (19)	0.69
Diabetes mellitus, n (%)	40 (41.2)	7 (33.3)	33 (43.4)	0.41
Coronary heart disease, n (%)	17 (17.5)	3 (14.3)	14 (18.4)	>0.99
Hypertlipidemia, n (%)	45 (46.4)	11 (52.4)	34 (44.7)	0.53
Smoking, n (%)	50 (51.5)	10 (47.6)	40 (52.6)	0.68
Previous stroke history, n (%)	31 (32.0)	10 (47.6)	21 (27.6)	0.08
Premorbid statin use <sup>a</sup> , n (%)	13 (13.4)	4 (19.0)	9 (11.8)	0.47
Onset-to-VWI time, days, median (IQR)	10 (9)	10 (7)	10 (9)	0.56
Admission NIHSS, median (IQR)	2 (3)	3 (4)	2 (2)	0.19
WBC, 10 <sup>9</sup> /L, median (IQR)	6.93 (2.06)	6.89 (3.15)	6.93 (1.83)	0.59
FBG, mmol/L, median (IQR)	5.95 (3.15)	5.90 (3.58)	5.97 (3.15)	0.53
TC, mmol/L, mean (SD)	4.52 (1.10)	4.79 (1.00)	4.44 (1.12)	0.20
HDL cholesterol, mmol/L, mean (SD)	1.00 (0.22)	1.04 (0.22)	0.99 (0.22)	0.42
LDL cholesterol, mmol/L, mean (SD)	3.05 (0.96)	3.23 (0.90)	3.00 (0.97)	0.32
TG, mmol/L, median (IQR)	1.50 (0.88)	1.50 (1.04)	1.53 (0.88)	0.55
Medication during follow-up				
Antihypertensive drug, n (%)	79 (81.4)	19 (90.5)	60 (78.9)	0.35
Statins, n (%)	60 (61.9)	13 (61.9)	47 (61.8)	>0.99
Antiplatelet drug, n (%)	33 (34.0)	10 (47.6)	23 (30.3)	0.14
Culprit plaque location				–
Anterior circulation, n (%)	69 (71.1)	14 (66.7)	55 (72.4)	
Intracranial internal carotid artery, n (%)	6 (6.2)	2 (9.5)	4 (5.3)	
Anterior cerebral artery, n (%)	3 (3.1)	0 (0.0)	3 (3.9)	
Middle cerebral artery, n (%)	60 (61.8)	12 (57.2)	48 (63.2)	

Variables	All participants (n = 97)	Recurrent participants (n = 21)	Non-recurrent participants (n = 76)	p value <sup>b</sup>
Posterior circulation, n (%)	28 (28.9)	7 (33.3)	21 (27.6)	
Basilar artery, n (%)	19 (19.6)	5 (23.8)	14 (18.4)	
Posterior cerebral artery, n (%)	9 (9.3)	2 (9.5)	7 (9.2)	
Recurrent stroke event	21	21	0	–
Stroke in the relevant artery territories	18 (85.7%)	18 (85.7%)	–	
Stroke in other artery territories	3 (14.3%)	3 (14.3%)	–	

SD standard deviation, IQR interquartile range, SBP systolic blood pressure, DBP diastolic blood pressure, VWJ vessel wall imaging, NIHSS National Institutes of Health Stroke Scale, WBC white blood cell, FBG fasting blood glucose, TC total cholesterol, HDL high-density lipoprotein, LDL low-density lipoprotein, TG triglyceride

<sup>a</sup> Pre-admission statin use was defined as regular statin medication use for more than a month before the index stroke

<sup>b</sup> Comparison between recurrent and non-recurrent stroke groups

Imaging features of the study sample

Table 2

Imaging features	All participants (n = 97)	Recurrent participants (n = 21)	Non-recurrent participants (n = 76)	p value <sup>a</sup>
HR-VWI features of culprit plaque				
Plaque burden, %, median (IQR)	75.00 (26.64)	84.00 (16.44)	69.35 (29.49)	0.001
Plaque volume, mm <sup>3</sup> , median (IQR)	42.83 (39.41)	41.02 (38.18)	43.41 (39.64)	0.96
Arterial remodeling ratio, median (IQR)	1.24 (0.64)	1.43 (0.69)	1.16 (0.61)	0.07
Positive remodeling, n (%)	67 (69.1)	17 (81.0)	50 (65.8)	0.18
Eccentric index, median (IQR)	0.58 (0.27)	0.57 (0.24)	0.59 (0.28)	0.78
Eccentricity, n (%)	63 (64.9)	14 (66.7)	49 (64.5)	0.85
Degree of stenosis, %, mean (SD)	49.84 (21.28)	59.82 (17.76)	47.08 (32.09)	0.01
Enhancement ratio, median (IQR)	1.55 (0.64)	1.62 (0.68)	1.53 (0.64)	0.56
Plaque enhancement, n (%)	77 (79.4)	18 (85.7)	59 (77.6)	0.55
Presence of HST1, n (%)	38 (39.2)	12 (57.1)	26 (34.2)	0.057
Total plaque numbers of each participant				
Intracranial plaque, median (IQR)	5 (3)	6 (2)	4 (3)	0.001
Intracranial enhanced plaque, median (IQR)	2 (3)	3 (2)	2 (2)	0.046
Intracranial plaques with HST1, median (IQR)	1 (1)	1 (0)	1 (1)	0.04
Extracranial carotid plaques, median (IQR)	0 (1)	1 (1)	0 (1)	0.03
Intracranial + extracranial carotid plaques, median (IQR)	5 (3)	6 (3)	5 (3)	0.001
Intracranial enhanced + extracranial carotid plaques, median(IQR)	3 (2)	4 (2)	3 (2)	0.01
Intracranial HST1 + extracranial carotid plaques, median (IQR)	1 (1)	2 (2)	1 (1)	0.002
Co-existing atherosclerosis				
Intracranial stenosis (> 50%) + extracranial carotid atherosclerosis, n (%)	27 (27.8)	13 (61.9)	14 (18.4)	<0.001
Intracranial + extracranial carotid atherosclerosis, n (%)	41 (42.3)	13 (61.9)	28 (36.8)	0.04
Intracranial enhanced + extracranial carotid atherosclerosis, n (%)	37 (38.1)	13 (61.9)	24 (31.6)	0.01
Intracranial HST1 + extracranial carotid atherosclerosis, n (%)	25 (25.8)	13 (61.9)	11 (14.5)	<0.001

HR-VWI/high-resolution vessel wall imaging, SD standard deviation, HST1 high signal on T1-weighted fat-suppressed images, IQR interquartile range

<sup>a</sup>Comparison between recurrent and non-recurrent stroke groups

Imaging features of the extracranial carotid plaques

**Table 3**

<b>Imaging features</b>	<b>Recurrent participants (n = 21)</b>	<b>Non-recurrent Participants (n = 76)</b>	<b>p value</b>
Maximal wall thickness, mm, median (IQR)	2.35 (0.91)	2.64 (1.72)	0.24
Plaque area, mm <sup>2</sup> , median (IQR)	19.08 (13.09)	22.65 (14.99)	0.71
Plaque burden, %, mean (SD)	54.60 (15.79)	55.13 (17.12)	0.82
Degree of stenosis, %, median (IQR)	13.77 (18.76)	12.38 (26.03)	0.67
Intraplaque hemorrhage, n (%)	3 (15.0)	8 (22.2)	0.73
Lipid-rich necrotic core, n (%)	3 (15.0)	11 (30.6)	0.20

*SD* standard deviation, *IQR* interquartile range

Univariable and multivariable Cox analysis to identify features associated with stroke recurrence

**Table 4**

Variables	Univariable Cox analysis with lasso selection			Multivariable Cox analysis		
	HR	95% CI	p value	HR	95% CI	p value
Age <sup>a</sup>	1.00	0.96–1.03	0.82	NA	NA	0.30
Male	0.93	0.39–2.25	0.87	NA	NA	0.67
Plaque burden <sup>b</sup>	1.66	1.21–2.28	0.002	NA	NA	0.050
Total plaque number of intracranial plaques	1.33	1.09–1.62	0.004	NA	NA	0.06
Co-existing intracranial stenosis (> 50%) + extracranial carotid atherosclerosis	4.89	2.02–11.80	< 0.001	NA	NA	0.38
Co-existing intracranial enhanced + extracranial carotid atherosclerosis	2.88	1.19–6.95	0.02	NA	NA	0.17
Co-existing intracranial HSTI + extracranial carotid atherosclerosis	6.12	2.52–14.82	0.001	6.12	2.52–14.82	0.001

HR hazard ratio, NA not available

<sup>a</sup>HR based on every 10-year increase

<sup>b</sup>HR based on every 10% increase